ACS Sustainable Chemistry & Engineering

Research Article

pubs.acs.org/journal/ascecg

Synthesis and Melt Processing of Sustainable Poly(ε-decalactone)-*block*-Poly(lactide) Multiblock Thermoplastic Elastomers

Mark T. Martello,[†] Deborah K. Schneiderman,[‡] and Marc A. Hillmyer*[,‡]

[†]Department of Chemical Engineering and Materials Science and [‡]Department of Chemistry, University of Minnesota, Minneapolis, Minnesota 55455-0431, United States

Supporting Information

ABSTRACT: A one-pot, one-catalyst, sequential ring-opening transesterification polymerization (ROTEP) was used to prepare fully renewable amorphous poly(D,L-lactide)−poly(ε-decalactone)−poly(D,L-lactide) (LDL) triblock polymers. These α,ω hydroxy-telechelic polymers were subsequently coupled to prepare linear alternating $(LDL)_n$ multiblock polymers. Differential scanning calorimetry (DSC) and small-angle X-ray scattering (SAXS) indicated microphase separation into two domains in both the triblock and multiblock architectures. The temperature dependent Flory−Huggins interaction parameter for this system, $\chi(T) = 69.1/T - 0.072$, was estimated from the experimentally determined order−disorder transition temperature (T_{ODT}) values of four symmetric LDL triblock polymers. Uniaxial extension tests revealed a dramatic dependence of the room-temperature mechanical properties on overall molar mass. Additionally, coupling low molar mass LDL triblocks to prepare $(LDL)_n$ multiblocks led to substantial increases in the ultimate elongation and tensile stress at break. Compared to high molar mass triblocks with inaccessible T_{ODT} values, $(LDL)_n$ multiblocks of similar composition and molar mass were found to disorder at much lower temperatures (T_{ODT} < 150 °C). Because of this, it was possible to process $(LDL)_n$ using injection molding. The simple synthetic procedure and melt processability of the $(LDL)_n$ multiblock polymers make these multiblocks attractive as renewable thermoplastic elastomers (TPEs).

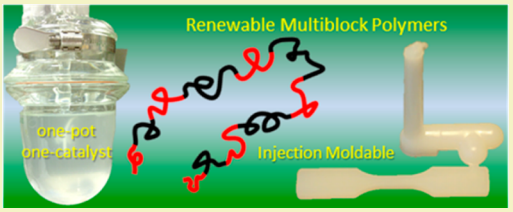

KEYWORDS: *Injection molding, Melt polymerization, Interaction parameter, Mechanical properties, Block polymers*

INTRODUCTION

Increased global awareness of the environmental consequences of traditional petroleum-derived plastics has driven the development of more sustainable alternatives including degradable polymers derived from renewable resources.[1−3] Although substantial research progress has been made in this area, the design of environmentally benign synthetic polymers is no trivial endeavor. In addition to the significant challenge of synthesizing and polymerizing new renewable monomers to produce novel high performance materials, chemists and engineers must consider the environmental impact, cost, and scalability of the manufacture and processing steps. Thermoplastic materials that are conducive to conventional processing techniques and can be prepared with low energy inputs using minimal solvents are especially desirable for reasons of both sustainability and cost.

Among numerous methods used to produce renewable polymers, sequential ring-opening transesterification polymerization (ROTEP) of bioderived lactones and cyclic diesters to form block polymers is particularly attractive due to ease of synthesis, versatility in monomer structure, and outstanding control over polymer molar mass and composition.[3,4] Many biologically derived lactone monomers have been successfully subjected to ROTEP to produce a variety of molecular architectures such homopolymers, statistical copolymers, and block polymers; some specific examples of bioderived lactone monomers include lactide, 1,5-dioxepan-2-one, δ-decalactone, ε-decalactone, menthide, and dihydrocarvide.[3,5−11] Lactide, a cyclic diester, is produced from the dimerization of the fermentation product lactic acid. The properties of poly(lactide) are greatly influenced by its tacticity. Atactic poly(lactide) (PLA) is an amorphous polymer with a glass transition temperature (T_g) up to 60 °C, while isotactic poly(L-lactide) (PLLA) is semicrystalline with a melting temperature (T_m) as high as 180 °C. ε-Decalactone (DL), an alkyl-substituted varient of ε-caprolactone, is prepared from castor oil and is commerically availible in its racemic form.[1112] Poly(ε-decalactone) (PDL) is amorphous with a low glass transition temperature ($T_g \approx -51$ °C).[10]

We and others have previously shown that an amorphous, low T_g, midblock in conjunction with PLA endblocks can be used to prepare ABA triblock thermoplastic elastomers (TPEs) with tunable mechanical properties.[13−20] While both amorphous and semicrystalline endblocks have been successfully employed, the equilibrium microstructure, mechanical properties, and minimum processing temperature can be drastically altered by endblock crystallinity. Additionally, the relatively high melting temperature of isotactic PLLA can preclude melt processing of polymers that also contain thermally unstable bonds, for example, urethane linkages.[21] Recent publications by

Received: June 27, 2014
Revised: August 31, 2014
Published: October 20, 2014

Scheme 1. Synthesis of Poly(ε -decalactone)-poly(lactide) Multiblock Polymers

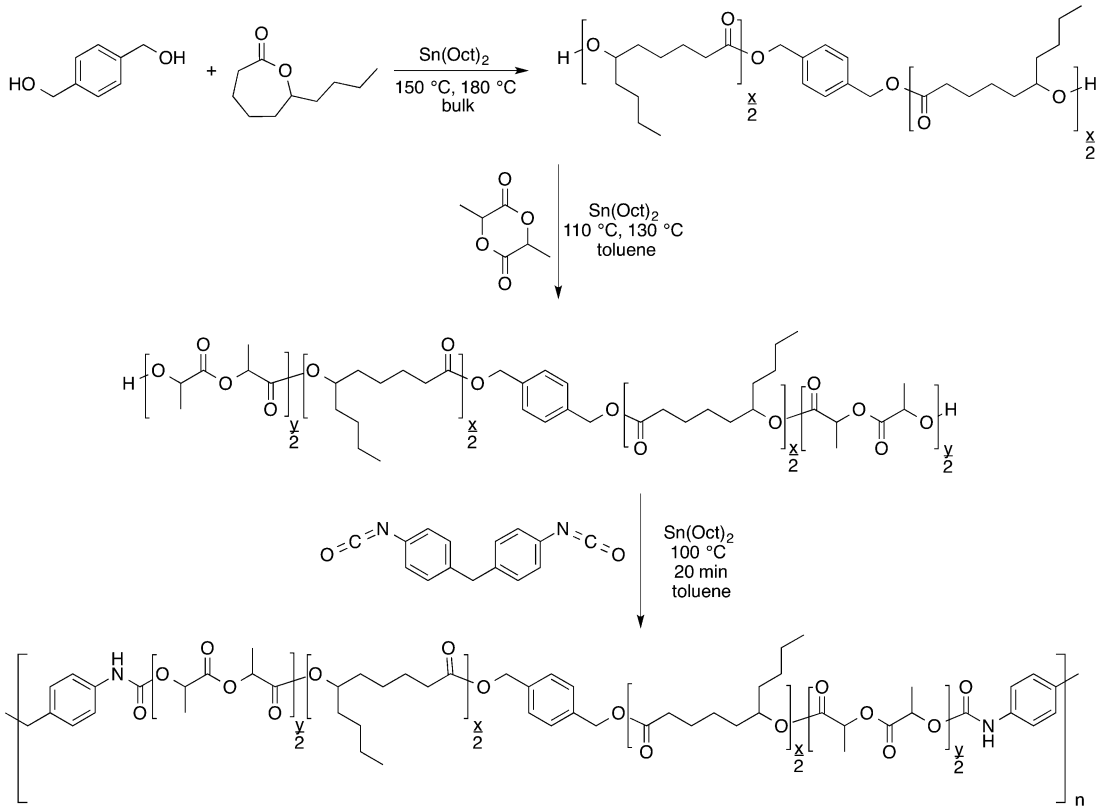

Olsén et al. regarding PLLA-*block*-PDL-*block*-PLLA triblock polymers and by Lin et al. concerning poly(ethylene glycol)-containing (PEG) PLLA-*block*-PDL-*block*-PEG-*block*-PDL-*block*-PLLA $(ABCBA)_n$ multiblock polymers suggest poly(ε-decalactone) may be an attractive midblock component for the synthesis of degradable lactide-based thermoplastic elastomers.[10,11] However, the mechanical properties of PDL-containing triblock and multiblock polymers have erstwhile only been reported for tough plastic materials with semicrystalline PLLA as a majority component.[11,10]

Previous investigations with a number of block polymer systems have revealed that significant increases in mechanical toughness can be effected by utilizing an $(AB)_n$ rather than a ABA architecture. This result that has been partially attributed to an increase in the fraction of rubbery chains that bridge multiple hard domains within the microphase separated material.[11,22−24] Beyond these mechanical advantages, the $(AB)_n$ architecture has the potential to address challenges associated with melt processing high molar mass materials. The viscosity of an ordered block polymer above the glass transition temperatures drops precipitously as the material is heated through the order−disorder transition temperature (T_{ODT}). To facilitate melt blending and high shear melt processing techniques such as injection molding, the preparation of block polymers with order−disorder transition temperatures well below the onset of thermal decomposition is desirable.[25] The decomposition temperature (T_D) is largely determined by the specific choice of polymer and end group functionality, whereas T_{ODT} is sensitive to composition, architecture, and molar mass.

The T_{ODT} values of ABA triblocks scale with the overall molar mass; this limits the molar mass of ABA triblocks amenable to melt processing to polymers that are untangled or only lightly entangled, that is, relatively weak materials.[26,27] Because the T_{ODT} values of $(AB)_n$ multiblock polymers are influenced more by the length of the repeating block than the total molar mass, it is possible to prepare high molar mass materials that are melt-processable by utilizing a multiblock architecture.[26] Olsén and co-workers established that the inclusion of ε-decalactone significantly increases the thermal stability of PDL containing block and statistical copolymers relative to PLLA. They demonstrated that PDL and PLLA are sufficiently immiscible for an ABA triblock (comprised of PLLA and PDL blocks of 20 and 40 kg mol^{-1}, respectively) to microphase separate.[10] Lin and colleagues describe their $(ABCBA)_n$ multiblock polymers as environmentally friendly thermoplastic elastomers; however, neither Lin et al. nor Olsén et al. investigated whether or not poly(ε-decalactone) block polymers are amenable to melt processing.[10,11] In this work, we describe the synthesis and phase behavior of amorphous PLA-*block*-PDL-*block*-PLA triblock and multiblock polymers and explore the effect of architecture on mechanical properties and melt processability of block polymers containing PDL as a majority component.

We report the preparation of linear [poly(lactide)-*block*-poly(ε-decalactone)]$_n$ multiblock polymers from the coupling of telechelic poly(lactide)-*block*-poly(ε-decalactone)-*block*-poly(lactide) triblocks with 4,4′-methylenebis(phenyl isocyanate) (MDI). We show that both polymerization and coupling can be conducted using tin(II) 2-ethylhexanoate ($Sn(oct)_2$) as a catalyst and that it is not necessary to isolate the intermediate during the process. We compare the properties of the multiblocks produced using this strategy to low molar mass triblock precursors and to high molar mass ABA triblocks that cannot be disordered prior to degradation. We demonstrate using injection molding that linear [poly(lactide)-*block*-poly(ε-

decalactone)]$_n$ (LDL)$_n$ multiblock polymers can be easily melt processed, this, together with the facile synthesis and improved mechanical properties relative to parent triblocks, make these renewable materials attractive new thermoplastic elastomers.

EXPERIMENTAL SECTION

Materials. ε-Decalactone (Sigma-Aldrich) was distilled under reduced pressure over calcium hydride and passed through a column of activated basic alumina (Sigma-Aldrich) without exposing it to air. Tin(II) 2-ethylhexanoate (Sigma-Aldrich) was distilled (3×) under reduced pressure and stored under dry nitrogen. 1,4-Benzenedimethanol (Sigma-Aldrich) was dried under reduced pressure at room temperature for 48 h. Toluene was purified by passing though activated alumina columns (Glass Contour, Laguna Beach, CA) prior to use. D,L-Lactide was generously provided by Ortec, Inc. (Easely, SC) and used as received. All of the reagents mentioned above were stored in a nitrogen filled glovebox. 4,4′-Methylenebis(phenyl isocyanate) (MDI) (Sigma-Aldrich) was stored at −20 °C and used as received. Chloroform (Fisher) and methanol (Fisher), used for polymer precipitation, were purchased and used without purification. Glass pressure vessels, Teflon caps, and Teflon-coated magnetic stir bars were stored in a 110 °C oven prior to being transferred to the glovebox. The reaction vessels were all charged and sealed in the glovebox and then quickly removed and placed in a heating bath. All other solvents were used as received without further purification. Although the acute toxicity of MDI is lower than many other organic cyanates, it is a known irritant, allergen, and sensitizer and is also a suspected carcinogen. Chloroform, used to dilute the polymers prior to precipitation, is toxic and a carcinogen. Methanol and toluene are both flammable. Toluene, chloroform, methanol, and MDI should be handled with caution in a well-ventilated area.

Characterization. ^{1}H NMR spectra were collected from deuterated chloroform solution on a Varian INOVA-500 spectrometer operating at 500 MHz. Chemical shifts are reported in δ (ppm) relative to the ^{1}H signals from residual protic solvent (7.26 ppm for $CHCl_3$). All ^{1}H NMR spectra are reported as the average of 100 scans and were acquired using a 5 s acquisition time and a 10 s delay. Size-exclusion chromatography (SEC) was conducted on a liquid chromatograph (Agilent 1100 series) equipped with a HP1047A refractive index detector. Polymer samples were diluted in chloroform (mobile phase) and passed through three Varian PLgel Mixed C columns at 35 °C under a constant volumetric flow rate (1 mL min^{-1}). Molar mass characteristics of the samples are referenced to polystyrene standards (Polymer Laboratories). Small-angle X-ray scattering (SAXS) experiments were conducted at the Advanced Photon Source (APS) of Argonne National Laboratories in sector 12-IDB.

Differential scanning calorimetry (DSC) was conducted on a TA Instruments Q-1000 DSC. Samples were analyzed in hermetically sealed aluminum pans. The samples were equilibrated at 100 °C and cooled to −100 at 10 °C min^{-1} followed by heating to 100 at 10 °C min^{-1}. Glass transition temperatures are reported upon the second heating cycle. The order−disorder transition temperatures were determined by dynamic mechanical analysis (DMA). Isochronal temperature ramps were conducted on a Rheometrics Scientific AR-G2 stress-controlled instrument between 25 mm parallel plates at an angular frequency of 1 rad s^{-1}. Dynamic strain sweeps were conducted at temperatures near the T_{ODT} to ensure the measurements were in the linear regime.

Injection molding was carried out using a Morgan Press G-55T injection molder equipped with an ASTM D638 Type D mold and an antidrool nozzle, which allows for compacting the melt in the barrel. Prior to loading the multiblock, the instrument was purged with a Dow Engage 8150. The instrument barrel was loaded with 55 g of multiblock. The loaded barrel holds 55 g, and each injection consumes ∼5 g of material. The runner and sprue sections of the part (3.5 g) were separated from the molded part and recycled. The instrument barrel was refilled after each injection and compacted to remove any air bubbles. The purge material from the first 4 injections was discarded, not recycled. The barrel temperature was initially 120 °C when the material was first loaded into the instrument and was decreased to 115 °C after part number 8 was injected. The nozzle temperature was kept +5 °C above the barrel temperature. Throughout the run the barrel temperature was increased in 5 steps to a maximum of 150 °C with each step comprising of 5 to 10 injections. The clamp, pilot, and ram pressure were 11 × 10^3, 6 × 10^3, and 5.5 × 10^3 psi, respectively. The ram pressure was held for 30 s from the start of the injection—the packing stage. After the ram was disengaged, the part was allowed to set for an additional 60 s prior to opening the mold and ejecting the part. Shortening the packing time resulted in the parts shrinking and the ejector pins deforming the sample.

Compression-molded samples were cut from a plaque of pressed material using a dog bone-shaped die; the specimen had dimensions of 10 mm (length) × 3 mm (width) × 1 mm (thickness). Tensile measurements of compression-molded materials were performed on a Shimadzu Autograph AGS-X Series tensile tester (Columbia, MD). Injection-molded samples were prepared using a ASTM D638 Type D mold and tested using an Instron Testing System (model 1011). All samples were elongated at a constant crosshead velocity of 50 mm min^{-1} until failure. The data for a minimum of 10 repetitions is shown in Figure 3; values are listed in Table S2 of the Supporting Information.

Representative Synthesis of LDL(11.8, 0.46) Triblock Polymer. In the glovebox, ε-decalactone (11.03 g, 64.7 mmol), Sn(Oct)$_2$ (23.5 mg, 58 μmol), and 1,4-benzenedimethanol (276.5 mg, 2.0 mmol) were added to a 48 mL pressure vessel equipped with a Teflon-coated magnetic stir bar. The sealed reaction vessel was placed in a 180 °C oil bath and stirred for 2 h before cooling to room temperature. The reaction vessel was returned to the glovebox to add D,L-lactide (12.5 g, 86.8 mmol) and toluene (16.62 g). The reaction was heated to 110 °C for 4 h after removal from the glovebox. The reaction solution was cooled to room temperature, diluted with dichloromethane, and precipitated in methanol (Sigma-Aldrich).

LDL(11.8, 0.46): ^{1}H NMR (500 MHz, chloroform-*d*) δ 0.88 (104 H, −C**H**$_3$) 1.11−1.41 (m, 205 H, −OC═O−CH$_2$CH$_2$C**H**$_2$CH$_2$CH-(CH$_2$C**H**$_2$C**H**$_2$CH$_3$)−O−) 1.42−1.77 (m, 491 H, −OC═O−CH$_2$**CH**$_2$CH$_2$**CH**$_2$CH(**CH**$_2$CH$_2$CH$_2$CH$_3$)−O− and −O−C═OCHC**H**$_3$−O−) 2.21−2.32 (m, 62 H, −OC═OC**H**$_2$−) 4.30−4.44 (m, 1.76 H, −C**H**(CH$_3$)−OH endgroup) 4.85 (quin, *J* = 5.8 Hz, 33 H, −C**H**(C$_4$H$_9$)−O−) 5.10 (s, 4.52 H, −C$_6$H$_4$C**H**$_2$− initiator) 5.12−5.33 (m, 84 H, −C**H**(CH$_3$)−O−) 7.34 (s, 4 H, Ar−**H** initiator).

Representative One-Pot Synthesis of (LDL)$_n$ (26.1, 0.28). A two-necked 100 mL round-bottomed flask was charged with ε-decalactone (52.06 g, 305.8 mmol), Sn(Oct)$_2$ (135 mg, 333 μmol), and benzenedimethanol (386 mg, 2.79 mmol) in a nitrogen-filled glovebox. The reaction vessel was removed from the glovebox and quickly fitted with an overhead stirrer under a purge of argon. After purging the headspace for 20 min, the reaction vessel was placed under 3−6 psig positive pressure of argon and submerged in a 180 °C oil bath. After 70 min, the reaction vessel was removed from the oil bath and allowed to cool. The reaction vessel was charged with D,L-lactide (28.01 g, 194.3 mmol), purged with argon, and placed in a 150 °C oil bath. After 40 min, the reaction was allowed to cool, toluene (65 mL) was added, and the polymer was dissolved while stirring at 100 °C for 40 min. MDI (0.8145 g, 3.25 mmol) was added followed by 25 mL of additional toluene. After 20 min, the reaction was cooled to room temperature, diluted in chloroform, and precipitated in methanol. After the residual solvent was removed under vacuum, 73.88 g of polymer were recovered for a gravimetric yield of 92%. (LDL)$_n$ (26.1, 0.28): ^{1}H NMR (500 MHz, chloroform-*d*) δ 0.88 (307 H, −C**H**$_3$) 1.1−1.4 (m, 615 H, −OC═O−CH$_2$CH$_2$C**H**$_2$CH$_2$CH-(CH$_2$C**H**$_2$C**H**$_2$CH$_3$)−O−) 1.43−1.75 (m, 1017 H, −OC═O−CH$_2$**CH**$_2$CH$_2$**CH**$_2$CH(**CH**$_2$CH$_2$CH$_2$CH$_3$)−O− and −O-C═OCHC**H**$_3$−O−) 2.2−2.45 (m, 203 H, −OC═OC**H**$_2$−) 3.88 (s, 1.87 H, −C**H**$_2$− MDI) 4.85 (quin, *J* = 5.9 Hz, 102 H, −C**H**(C$_4$H$_9$)−O−) 5.10 (s, 4.89 H, −C$_6$H$_4$C**H**$_2$− initiator) 5.12−5.35 (m, 122 H, −C**H**(CH$_3$)−O−) 7.09 (m, 4.45 H, Ar−**H** MDI) 7.34 (s, 4 H, Ar−**H** initiator)

dx.doi.org/10.1021/sc500412a | ACS Sustainable Chem. Eng. 2014, 2, 2519−2526

RESULTS AND DISCUSSION

We first investigated the impact of temperature, initiator concentration, and catalyst concentration on the tin(II) octoate-catalyzed bulk polymerization of ε-decalactone. Whereas polymerizations conducted at 130 °C with moderate catalyst loadings ($[DL]_o/[Sn(Oct)_2]$ = 500) typically reached ∼95% conversion only after 22 h, an increase in reaction temperature to 180 °C resulted in monomer conversions of up to 99% after only 2−4 h at a much lower catalyst loading ($[DL]_o/[Sn(Oct)_2]_o$ = 1000) (Table S1, Supporting Information). Under these conditions, the number−average molar mass (M_n) determined by ^{1}H NMR spectroscopy and the calculated theoretical M_n were in excellent agreement. Furthermore, the dispersity determined by size-exclusion chromatography (SEC) relative to polystyrene standards was narrow. Taken together, these data indicate essentially quantitative initiation and well-controlled polymerization by a chain growth mechanism.

ABA triblock polymers were prepared by the addition of D,L-lactide to α,ω-dihydroxy telechelic poly(ε-decalactone) macroinitiators in the presence of $Sn(Oct)_2$ at 110 °C; polymer compositions were easily controlled by adjusting the weight fraction of lactide to difunctional PDL. This chain extension was successfully conducted in the melt. Alternatively, one mass equivalent of toluene could be added to lower the viscosity of the mixture and facilitate mixing. After 4 h at 110 °C or 2 h at 130 °C, the triblocks were diluted with chloroform and purified by precipitation in methanol. Among numerous potential green alternatives to chloroform, it is possible that lactate esters, methyl acetate, or dimethoxyethane are viable.[28] Compared to the PDL macroinitatior, the SEC chromatograms for the triblock show an obvious shift to higher molar mass. The dispersity of the triblocks remained reasonably narrow ($Đ$ = 1.1−1.3) with no evidence of uninitiated PDL or PLA homopolymer (Figure 1).

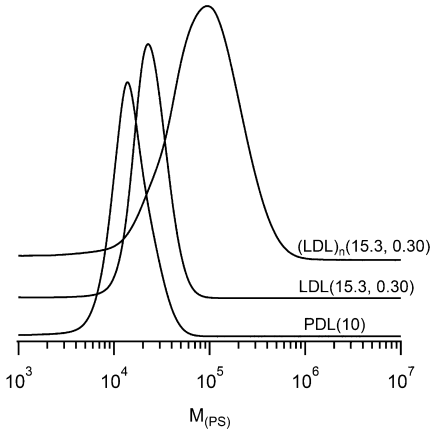

Figure 1. Representative sequence of size-exclusion chromatograms for PDL (10 kg mol^{-1}), LDL(15.3, 0.30), and $(LDL)_n$(15.3, 0.30). The LDL and $(LDL)_n$ chromatograms are shown for the purified polymers. The value of n for $(LDL)_n$(15.3, 0.30) is 4.6.

The multiblock polymers were prepared by linking α,ω-hydroxy telechelic LDL triblock polymers using MDI as a coupling agent in the presence of catalytic $Sn(Oct)_2$. The average number of triblock polymers per multiblock chain, n, was calculated from the ratio of the number-average molar mass determined using SEC (M_n^{SEC}) of multiblock to the triblock. The characteristics of several LDL triblocks and $(LDL)_n$ multiblocks are summarized in Table 1.

Differential scanning calorimetry (DSC) was used to determine the glass transition temperatures of PDL homopolymers, LDL triblocks, and $(LDL)_n$ multiblock polymers; representative thermograms are shown in Figure S1 of the Supporting Information. Each of the LDL and $(LDL)_n$ block polymers studied exhibit two glass transition temperatures—one below −38 °C and the other above 31 °C—which we attribute to microphase separation into PDL- and PLA-rich domains, respectively. Whereas the T_g values of the triblock PLA segments are in fair agreement with those predicted for PLA homopolymer of the same molar mass, the T_g values of the PDL segments deviate positively from pure PDL (Figure S2, Supporting Information).[31,32] This departure from Flory−Fox behavior is indicative of increased PLA in the PDL-domain as the molar mass of the PDL blocks is decreased and is consistent with many previously reported block polymer systems.[13,23,24,33−36]

The microstructures of LDL and $(LDL)_n$ block polymers were investigated using small-angle X-ray scattering (SAXS). As indicated by the solid triangles in Figure 2, both LDL and $(LDL)_n$ samples exhibited strong principal peaks (q^*) at low q corresponding to principle domain spacing in the range of 12.2−43.2 and 12.1−18.9 nm for the triblocks and multiblocks, respectively. LDL triblock samples with nearly symmetric compositions displayed higher order peaks at odd integer values of q, which are the expected locations for a lamellar morphology with systematic structure factor extinctions (Figure S3, Supporting Information). While the morphology of the two highest molar mass triblocks LDL(136, 0.21) and LDL(148, 0.27) could not be determined from the SAXS data, a lower molar mass PLA-*block*-PDL diblock of similar composition showed well-defined higher order reflections consistent with the expected hexagonally close-packed cylinder morphology (Figure S3, Supporting Information).[37] The $(LDL)_n$ multiblock samples exhibited strong principal reflections; however, for most samples, a definitive assignment of morphology was not possible due to broad low intensity higher order reflections. This is unsurprising because as molar mass and the number of blocks per chain increases the ability of the system to equilibrate into a long-range ordered system becomes increasingly difficult.[38]

In block polymers, the microphase separation of disparate components to form ordered morphologies is governed by the total number of repeat units (N), the volume fraction of each component (f), and the segment−segment interaction parameter (χ). For compositionally symmetric ABA triblocks, random phase approximation theory predicts the position of the lamellar to disorder phase boundary at $(\chi N)_{ODT}$ = 17.996. From this relationship, the temperature dependence of χ can be estimated using the T_{ODT} values of compositionally symmetric (f_{PLA} = 0.5) triblocks with known N.[37] In this work, we assume the temperature dependence of χ can be described by eq 1:

$$\chi(T) = \frac{\alpha}{T} + \beta \quad (1)$$

In this equation, α and β represent the excess enthalpic and entropic contributions to the energy of mixing the blocks, respectively. We determined the order−disorder transition temperatures of LDL and $(LDL)_n$ using dynamic mechanical analysis (DMA) at low strain. T_{ODT} was taken as the onset of the discontinuous drop in the storage modulus (G') upon

Table 1. Characteristics of Poly(lactide)-*block*-poly(ε-decalactone)-*block*-poly(lactide) Triblock and Multiblock Polymers

	block M_n^{NMR}									
triblock[a]	PLA[b] (kg mol^{-1})	PDL (kg mol^{-1})	M_n^{SEC} (kg mol^{-1})[c]	$Đ$[c]	N_{tot}[d]	f_{PLA}[d]	D[e] (nm)	T_g^{PDL} (°C)	T_g^{PLA} (°C)	T_{ODT} (°C)[f]
LDL(10.0, 0.46)	2.6	4.8	14.3	1.18	128	0.46	12.2	−44	32	51
LDL(11.3, 0.51)	3.2	4.9	17.9	1.19	143	0.51	14.4	−44	31	80
LDL(11.8, 0.46)	3.1	5.6	18.5	1.17	151	0.46	13.6	−44	33	93
LDL(12.8, 0.46)	3.3	6.1	20.9	1.17	164	0.46	14.4	−45	36	102
LDL(15.3, 0.30)	2.7	9.9	25.6	1.18	190	0.30	15.1	−46	35	65
LDL(18.9, 0.51)	5.4	8.2	32.0	1.30	239	0.51	21.5	−47	44	n.d.
LDL(136, 0.21)	18	100	170	1.33	1910	0.21	33.8	−49	55	
LDL(148, 0.27)	24	100	206	1.28	1990	0.27	43.2	−49	54	
	block M_n^{NMR}									
multiblock[a]	PLA[b] (kg mol^{-1})	PDL (kg mol^{-1})	M_n^{SEC} (kg mol^{-1})[c]	$Đ$	n[g]	f_{PLA}[d]	D[e] (nm)	T_g^{PDL} (°C)	T_g^{PLA} (°C)	T_{ODT} (°C)[f]
$(LDL)_n$(10.0, 0.46)	2.6	4.8	71	1.68	5.0	0.46	12.1	−38	33	70
$(LDL)_n$(13.4, 0.27)[h]	2.2	9.1	151	2.13	4.9	0.27	13.4	−46		110
$(LDL)_n$(15.3, 0.30)	2.7	9.9	117	1.80	4.6	0.30	14.9	−46	54	108
$(LDL)_n$(16.0, 0.23)[h]	2.2	11.6	173	2.08	5.6	0.23	15.3	−46	41	112
$(LDL)_n$(18.4, 0.19)[h]	2.1	14.2	219	2.45	6.0	0.19	18.9	−47	47	140

[a]PLA-*b*-PDL-*b*-PLA triblock polymers are abbreviated as LDL(*x*,*y*), where *x* is the total M_n of the triblock in kg mol^{-1}, and *y* is the volume fraction of PLA (f_{PLA}). $(PLA\text{-}b\text{-}PDL\text{-}b\text{-}PLA)_\eta$ multiblock polymers abbreviated similarly as $(LDL)_n$(*x*,*y*), where *x* is the M_n of the triblock repeat unit, and *y* is the volume fraction of PLA (f_{PLA}). [b]Molar mass reported for PLA block or 1/2 the total molar mass of PLA per chain. [c]Relative molar mass and dispersity based on polystyrene standards. [d]N_{TOT} and f_{PLA} are calculated using room temperature densities of PLA[29] (1.24 g cm^{-3}) and PDL[30] (0.97 g cm^{-3}). N_{TOT} is calculated from the sum of the number-average molar mass of the component blocks (M_n^{NMR}) using a reference volume of 118 Å^3. [e]Principal domain spacing of the bulk sample determined by SAXS at room temperature. [f]T_{ODT} values determined by dynamic mechanical analysis. while heating at a rate of 1 °C min^{-1}. The T_{ODT} is taken as the onset of the rapid discontinuous drop in G'. [g]Average triblock number determined by M_n^{SEC} of multiblock relative to the precursor triblock. [h]Precursor triblocks were not isolated. A small aliquot was taken for SEC analysis prior to the coupling reaction.

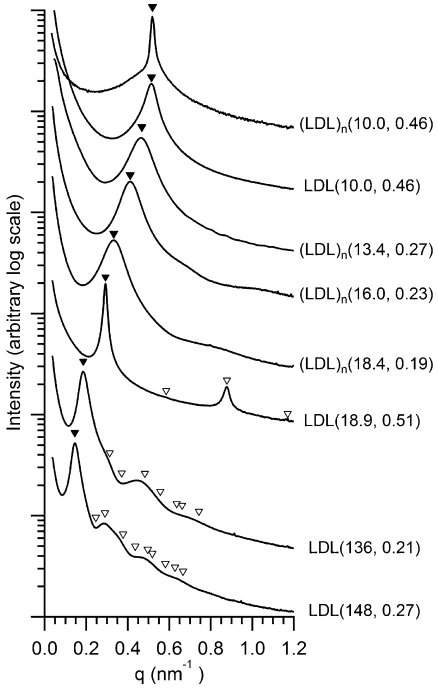

Figure 2. Room temperature SAXS patterns for select LDL triblocks and $(LDL)_n$ multiblocks. The principal peaks at low *q* are indicated with the solid triangles (▼), and the open triangles (▽) indicate the position of the allowed higher order reflections. LDL(136, 0.21) and LDL(148, 0.27) are indexed for hexagonally packed cylinders, and LDL(18.9, 0.51) is indexed for alternating lamella.

isochronal (ω = 1 rad s^{-1}) heating at a rate of 0.8 °C min^{-1} (Figures S4 and S5, Supporting Information). For several low molar mass LDL triblocks, these results were corroborated using DSC (Figures S5 and S6, Supporting Information).[39] On the basis of the measured order−disorder transition temperatures of compositionally symmetric LDL triblock polymers, we estimated the temperature dependence of χ for the PLA−PDL system using eq 2 (Figure S7, Supporting Information)

$$\chi_{PLA-PDL} = \frac{(69.1 \pm 9.2)}{T} - (0.072 \pm 0.026) \quad (2)$$

For this work, the overall degree of polymerization, *N*, was calculated based on a standard reference volume of 118 Å^3 using the room temperature densities of the respective homopolymers.[40,29,30] Direct comparison of the χ value based on the aliphatic character and monomer structure can be made between $\chi_{PLA-PMCL}$ and $\chi_{PLA-PDL}$; exchanging the methyl group of poly(ε-methyl-ε-caprolactone) (PMCL) for a *n*-butyl group on PDL results in a 2-fold increase in χ at 140 °C.[13]

Room temperature uniaxial extension experiments were conducted to evaluate the mechanical properties of LDL triblock and $(LDL)_n$ multiblock polymers. Dog bone-shaped specimens, prepared by compression molding at temperatures above the T_g of the PLA domain, were elongated at constant crosshead velocity of 50 mm min^{-1} until failure. The data for a minimum of 10 repetitions is listed in Table S2 of the Supporting Information, and representative engineering stress−strain curves are shown in Figure 3. Notably, LDL(148, 0.27), is mechanically similar to previously reported amorphous poly(lactide)-*block*-poly(6-methyl-ε-caprolactone)-*block*-poly(lactide) triblocks but weaker than several previously reported ABA triblocks containing semicrystalline PLLA.[19,20] A lower molar mass sample of similar composition, LDL(15.3, 0.30), is characterized by a comparatively low tensile strength (σ_t) and strain at break (ε_b) (σ_t = 0.24 MPa, ε_b = 218%, and σ_t = 9.4 MPa, ε_b = 1310% for LDL(15.3, 0.3) and LDL(148, 0.27), respectively). It is likely that poor mechanical properties of the

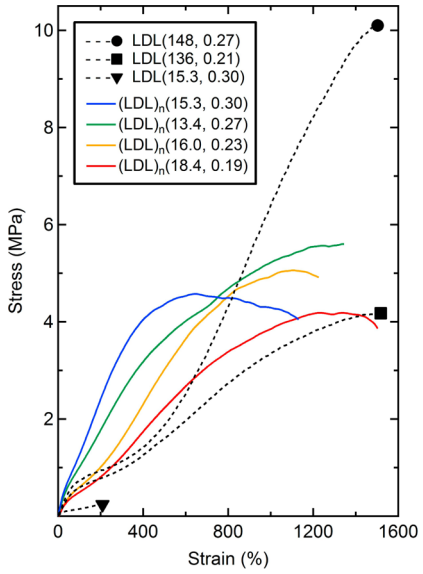

Figure 3. Representative stress−strain traces for LDL triblock (black) and $(LDL)_n$ multiblock polymers (colors). The samples were prepared by compression molding a uniform sheet at the temperatures listed in Table S2 of the Supporting Information.

low molar mass triblock are partially due to the failure of the unentangled PLA-domains to act effectively as hard physical cross-links. Both the low molar mass of the PLA blocks and the proximity of the PLA glass transition to the testing temperature (35 and 20 °C, respectively) suggest failure by a chain pullout mechanism.[22,41−43]

Although the molar masses of the individual segments are still insufficient for significant entanglement to occur, the mechanical properties are vastly improved in the $(LDL)_n$(15.3, 0.30), multiblock compared to LDL(15.3, 0.30).[44] Upon coupling, σ_t increases an order of magnitude and ε_b by a factor of 5; these increases can be attributed to both the block architecture and the doubled molar mass of the internal PLA domains.[11,22−24,26] The increased block number allows a single chain to bridge multiple domains, enhancing the connectivity of the physically cross-linked network. The doubled molar mass of the internal PLA blocks within the multiblock leads to a substantial increase in the glass transition of the PLA domain, increasing the strength of the hard physical cross-links in the material.

Although the highest molar mass LDL triblock is tougher than $(LDL)_n$ multiblocks, the T_{ODT} of the triblock is estimated to be 390 °C, higher than the decomposition temperature.[10] As previously reported by Wu et al. for the case of [poly(styrene)-*block*-poly(isoprene)]$_n$ multiblocks, as the number of blocks in an $(AB)_n$ increases, the T_{ODT} approaches an asymptotic maximum value.[26] This result is consistent with random phase approximation and self-consistent mean field theory, which predict that the maximum T_{ODT} can be estimated using χ and the degree of polymerization of the repeating AB unit.[26,37] These results imply that the T_{ODT} of a $(LDL)_n$ multiblock should be substantially lower than a LDL triblock of the same composition and molar mass but higher than the T_{ODT} of the constituent prepolymer, which was coupled to make it. This was confirmed in the current work using dynamic mechanical analysis of LDL(15.3, 0.30) and $(LDL)_n$(15.3, 0.30). As indicated in Figure S8 of the Supporting Information, the order−disorder transition temperature for these samples were found to be 65 and 108 °C, respectively. The DMA data for an array of $(LDL)_n$ multiblocks are shown in Figure S5 of the Supporting Information; the T_{ODT} values are listed in Table 1.

Upon heating through the order−disorder transition temperature, the modulus of the LDL(15.3, 0.30) drops almost a decade within 10 °C; over this temperature range, the modulus of the multiblock is much less sensitive to temperature. Whereas the $(LDL)_n$(15.3, 0.30) multiblock also exhibits a rapid drop in G' above the T_{ODT}, the change occurs over a broader range of temperature; similar broad transitions have previously been observed for other multiblock systems.[23,26] The breadth of the multiblock T_{ODT} is likely due to the broad dispersity, specifically the presence of high molar mass species resulting from the coupling reaction. The extremely long relaxation times for these species would require experimental frequencies below the limits of the instrument to allow these large chains to fully relax within the time scale of the experiment.[26]

The relatively low T_{ODT} of $(LDL)_n$(15.3, 0.30) made this sample an attractive candidate for the melt processing. To illustrate the efficacy of this, we used injection molding with a laboratory-scale ram and barrel type instrument to prepare dog bone-shaped tensile bars. In this process, the material was heated in the barrel to a temperature above the T_{ODT} and then injected into a lower temperature dog bone-shaped mold. After the parts were ejected from the mold, the sprue and runner section was separated from the tensile bar and recycled back into the barrel (Figure 4). Despite preprocessing and recycling steps, SEC comparison of the molded parts to the pristine material revealed minimal degradation (Figure S9, Supporting Information).

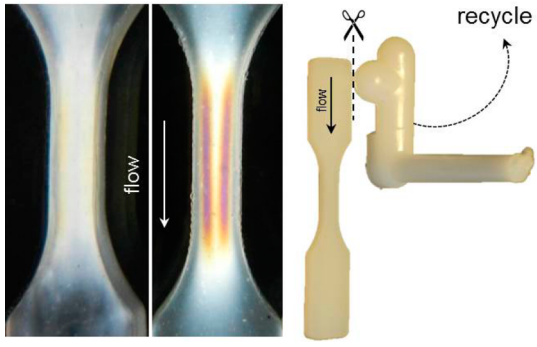

Figure 4. Representative image of the gauge of an injection-molded part under cross-polarized light. The image on the left is a sample molded with barrel and mold temperatures of 124 and 44 °C, respectively. The image on the right is a sample molded with barrel and mold temperatures of 149 and 36 °C, respectively. The parallel colored bands spanning the gauge are indicative of thermal stresses formed during the rapid cooling of the part. This region has the smallest cross-sectional area and is the area of the sample that cools most rapidly. The bright band extending vertically the length of the image, in the direction of flow, and horizontally nearly the width of the sample is attributed to birefringence caused by domain alignment.

Injection-molded parts of $(LDL)_n$(15.3, 0.30) were subjected to uniaxial extension at a constant crosshead velocity of 50 mm min^{-1} until failure of the sample. Compared to compression-molded samples, the injection-molded parts showed a 45% improvement in the tensile strength. At small strain, the injection-molded material had a higher modulus than either of the compression-molded materials. (Table S2, Figure S10,

Supporting Information) Encouragingly, the set and ultimate strains of the injection-molded multiblock is comparable to commercial styrenic TPEs (Table S3, Supporting Information).[45]

When imaged under cross-polarized light, the injection-molded parts showed bright white regions indicative of birefringence due to chain alignment (Figure 4). Some parts also showed parallel dark bands extending the length of the gauge; these features were most prevalent in the parts injected with the highest difference between the melt and mold temperatures and are likely due to residual thermal stresses (Figure S11, Supporting Information). By comparing the tensile run-to-run variation with the polarized images, the presence of residual thermal stresses did not appear to significantly alter the tensile behavior. The difference in the stress−strain behavior at high strain between the injection-molded and compression-molded samples is attributed to domain alignment; these observations are consistent with observed behavior of sytrenic block polymer systems.[46−48]

CONCLUSIONS

We have demonstrated the preparation of LDL triblocks in the melt using a one-pot one-catalyst method. By coupling LDL triblocks with MDI, we consistently obtained $(LDL)_n$ multiblock polymers with n close to 5 (undecablock) and a dispersity close to 2. The bulk properties of the triblock and multiblock polymers were analyzed by DSC, SAXS, DMA, and uniaxial extension experiments. Microphase separation was suggested by DSC data for both the triblock and multiblock polymers and corroborated by SAXS. The order−disorder transition temperatures of four LDL triblocks were used to estimate the temperature dependent segment−segment interaction parameter between PLA and PDL.

Highly segregated high molar mass LDL triblocks exhibited impressive tensile toughness; however, the T_{ODT} values of these polymers could not be accessed prior to degradation. $(LDL)_n$ multiblocks with similar composition and total molar mass were found to have T_{ODT} values below 150 °C. These polymers were amenable to a high shear melt processing; this was demonstrated by injection molding a $(LDL)_n$ multiblock polymer to form dog bone-shaped parts. Compared to the compression-molded material, a slight increase in toughness was observed in the injection-molded parts, an effect potentially due to shear-induced domain alignment. The combined properties of the $(LDL)_n$ multiblock polymers make these materials attractive new renewable thermoplastic elastomers.

ASSOCIATED CONTENT

Supporting Information

Tables S1−S3 and Figures S1−S12. This material is available free of charge via the Internet at http://pubs.acs.org.

AUTHOR INFORMATION

Corresponding Author

*E-mail: hillmyer@umn.edu.

Notes

The authors declare no competing financial interest.

ACKNOWLEDGMENTS

SAXS data were acquired at Sector 12 IDB of the Advanced Photon Source (APS), additional experiments were conducted at the Dupont−Northwestern−Dow Collabrative Access Team (DND CAT) located at Sector 5 of the APS. DND Cat is supported by L.E. Dupont de Nemours and Co., The Dow Chemical Co., and the State of Illinois. Use of the APS was supported by the U.S. Department of Energy, Office of Science, Office of Basic Energy Sciences, under Contract No. DE-AC02-06CH11357. Partial funding for this work was provided by the Center for Sustainable Polymers at the University of Minnesota, a National Science Foundation (NSF)-supported Center for Chemical Innovation (CHE-1413862). M.M. thanks Sangwoo Lee and Frank Bates for helpful discussions as well as David Giles and Chris Macosko for their introduction to injection molding.

ABBREVIATIONS:

DMA:dynamic mechanical analysis
DSC:differential scanning calorimetry
^{1}H NMR:proton nuclear magnetic resonance spectroscopy
LDL:poly(D,L-lactide)−poly(ε-decalactone)−poly(D,L-lactide) triblock polymer
$(LDL)_n$:(poly(D,L-lactide)−poly(ε-decalactone)−poly(D,L-lactide))$_n$ multiblock
PLA:poly(D,L-lactide)
PD:poly(ε-decalactone)
ROTEP:ring-opening transesterification polymerization
SAXS:small-angle X-ray scattering
SEC:size-exclusion chromatography
TPE:thermoplastic elastomers
T_D:degradation temperature
T_g:glass transition temperature
T_{ODT}:order to disorder transition temperature

REFERENCES

(1) Gandini, A. The irruption of polymers from renewable resources on the scene of macromolecular science and technology. *Green Chem.* **2011**, *13*, 1061−1083.
(2) Ragauskas, A. J.; Williams, C. K.; Davison, B. H.; Britovsek, G.; Cairney, J.; Eckert, C. A.; Frederick, W. J.; Hallett, J. P.; Leak, D. J.; Liotta, C. L.; et al. The path forward for biofuels and biomaterials. *Science* **2006**, *311*, 484−489.
(3) Lindblad, M. S.; Liu, Y.; Albertsson, A.-C.; Ranucci, E.; Karlsson, S. Degradable aliphatic polyesters; polymers from renewable resources. *Adv. Polym. Sci.* **2000**, *157*, 139−161.
(4) Albertsson, A. C.; Varma, I. K. Aliphatic polyesters: Synthesis, properties and applications. *Adv. Polym. Sci.* **2002**, *157*, 1−40.
(5) Martello, M. T.; Burns, A.; Hillmyer, M. Bulk ring-opening transesterification polymerization of the renewable δ-decalactone using an organocatalyst. *ACS Macro Lett.* **2012**, *1*, 131−135.
(6) Lowe, J. R.; Martello, M. T.; Tolman, W. B.; Hillmyer, M. A. Functional biorenewable polyesters from carvone-derived lactones. *Polym. Chem.* **2011**, *2*, 702.
(7) Lowe, J. R.; Tolman, W. B.; Hillmyer, M. a. Oxidized dihydrocarvone as a renewable multifunctional monomer for the synthesis of shape memory polyesters. *Biomacromolecules* **2009**, *10*, 2003−2008.
(8) Zhang, D.; Hillmyer, M. A.; Tolman, W. B. Catalytic polymerization of a cyclic ester derived from a "cool" natural precursor. *Biomacromolecules* **2005**, *6*, 2091−2095.
(9) Pitt, C. G.; Gratzl, M. M.; Kimmel, G. L.; Surles, J.; Schindler, A. Aliphatic polyesters II. The degradation of poly (D,L-lactide), poly (ε-caprolactone), and their copolymers in vivo. *Biomaterials* **1981**, *2*, 215−220.
(10) Olsén, P.; Borke, T.; Odelius, K.; Albertsson, A.-C. ε-Decalactone: A thermoresilient and toughening comonomer to poly(L-lactide). *Biomacromolecules* **2013**, *14*, 2883−2890.

(11) Lin, J.-O.; Chen, W.; Shen, Z.; Ling, J. Homo- and block copolymerizations of ε-decalactone with L-lactide catalyzed by lanthanum compounds. *Macromolecules* **2013**, *46*, 7769−7776.
(12) Romero-Guido, C.; Belo, I.; Ta, T.; Cao-Hoang, L.; Alchihab, M.; Gomes, N.; Thonart, P.; Teixeira, J.; Destain, J.; Waché, Y. Biochemistry of lactone formation in yeast and fungi and its utilisation for the production of flavour and fragrance compounds. *Appl. Microbiol. Biotechnol.* **2011**, *89*, 535−547.
(13) Martello, M. T.; Hillmyer, M. A. Polylactide−poly(6-methyl-ε-caprolactone)−polylactide thermoplastic elastomers. *Macromolecules* **2011**, *44*, 8537−8545.
(14) Wanamaker, C. L.; O'Leary, L. E.; Lynd, N. A.; Hillmyer, M. A.; Tolman, W. B. Renewable-resource thermoplastic elastomers based on polylactide and polymenthide. *Biomacromolecules* **2007**, *8*, 3634−3640.
(15) Frick, E. M.; Zalusky, A. S.; Hillmyer, M. A. Characterization of polylactide-*b*-polyisoprene-*b*-polylactide thermoplastic elastomers. *Biomacromolecules* **2003**, *4*, 216−223.
(16) Sipos, L.; Zsuga, M.; Deak, G.; Deák, G. Synthesis of poly(L-lactide)-*block*-polyisobutylene-*block*-poly(L-lactide): A new biodegradable thermoplastic elastomer. *Macromol. Rapid Commun.* **1995**, *16*, 935−940.
(17) Zhang, S.; Hou, Z.; Gonsalves, K. E. Copolymer synthesis of poly(L-lactide-*b*-DMS-*b*-L-lactide) via the ring opening polymerization of L-lactide in the presence of α,ω-hydroxylpropyl-terminated PDMS macroinitiator. *J. Polym. Sci., Part A: Polym. Chem.* **1996**, *34*, 2737−2742.
(18) Zhang, Z.; Grijpma, D. W.; Feijen, J. Triblock copolymers based on 1,3-trimethylene carbonate and lactide as biodegradable thermoplastic elastomers. *Macromol. Chem. Phys.* **2004**, *205*, 867−875.
(19) Ryner, M.; Albertsson, A.-C. Resorbable and highly elastic block copolymers from 1,5-dioxepan-2-one and L-lactide with controlled tensile properties and hydrophilicity. *Biomacromolecules* **2002**, *3*, 601−608.
(20) Xiong, M.; Schneiderman, D. K.; Bates, F. S.; Hillmyer, M. A.; Zhang, K. Scalable production of mechanically tunable block polymers from sugar. *Proc. Natl. Acad. Sci. U.S.A.* **2014**, *111*, 8357−8362.
(21) Ulrich, H. Polyurethane stabilizers. *J. Elastomers Plast.* **1986**, *18*, 147−158.
(22) Matsumiya, Y.; Watanabe, H.; Takano, A.; Takahashi, Y. Uniaxial extensional behavior of $(SIS)_p$-type multiblock copolymer systems: Structural origin of high extensibility. *Macromolecules* **2013**, *46*, 2681−2695.
(23) Lee, I.; Panthani, T. R.; Bates, F. S. Sustainable poly(lactide-*b*-butadiene) multiblock copolymers with enhanced mechanical properties. *Macromolecules* **2013**, *46*, 7387−7398.
(24) Lee, I.; Bates, F. S. Synthesis, structure, and properties of alternating and random poly(styrene-*b*-butadiene) multiblock copolymers. *Macromolecules* **2013**, *46*, 4529−4539.
(25) Drobny, J. G., *Handbook of Thermoplastic Elastomers*; Plastics Design Library; Elsevier Science: New York, 2007.
(26) Wu, L.; Cochran, E. W.; Lodge, T. P.; Bates, F. S. Consequences of block number on the order−disorder transition and viscoelastic properties of linear $(AB)_n$ multiblock copolymers. *Macromolecules* **2004**, *37*, 3360−3368.
(27) Tong, J.-D.; Jerôme, R.; Jerome, R. Dependence of the ultimate tensile strength of thermoplastic elastomers of the triblock type on the molecular weight between chain entanglements of the central block. *Macromolecules* **2000**, *33*, 1479−1481.
(28) Benazzouz, A.; Moity, L.; Pierlot, C.; Sergent, M.; Molinier, V.; Aubry, J. Selection of a greener set of solvents evenly spread in the hansen space by space-filling design. *Ind. Eng. Chem. Res.* **2013**, *52*, 1685−1697.
(29) Anderson, K. S.; Hillmyer, M. A. Melt chain dimensions of polylactide. *Macromolecules* **2004**, *37*, 1857−1862.
(30) The density of PDL is reasonably approximated by density of poly(δ-decalactone) reported in reference 5.
(31) Jamshidi, K.; Hyon, S.-H.; Ikada, Y. Thermal characterization of polylactides. *Polymer* **1988**, *29*, 2229−2234.
(32) The systematically higher T_g in the LDL triblocks is due to a difference in measurement technique between our work and that of reference 30 rather than an actual elevation of the T_g of the lactide domain of the triblock. In this work, we have used the inflection point to define the glass transition, which we believe gives more consistent results in cases where the glass transition is broad and the onset not sharply defined.
(33) Granger, A. T.; Krause, S.; Fetters, L. J. Phase-mixing effect in styrene-butadiene block copolymers. *Macromolecules* **1987**, *20*, 1421−1423.
(34) Lu, Z.; Krause, S. Properties of low-molecular weight block copolymers 0.2. Refractive index-temperature measurements of styrene-dimethylsiloxane diblock copolymers. *Macromolecules* **1982**, *15*, 112−114.
(35) Wang, B. Y.; Krause, S. Properties of dimethylsiloxane microphases in phase-separated dimethylsiloxane block copolymers. *Macromolecules* **1987**, *20*, 2201−2208.
(36) Krause, S.; Iskandar, M.; Iqbal, M. Properties of low-molecular weight block copolymers 0.1. Differential scanning calorimetry of styrene-dimethylsiloxane diblock copolymers. *Macromolecules* **1982**, *15*, 105−111.
(37) Matsen, M. W. Effect of architecture on the phase behavior of AB-type block copolymer melts. *Macromolecules* **2012**, *45*, 2161−2165.
(38) Krause, S. Microphase separation in block copolymers. Zeroth approximation including surface free energies. *Macromolecules* **1970**, *3*, 84−86.
(39) Lee, S.; Gillard, T. M.; Bates, F. S. Fluctuations, order, and disorder in short diblock copolymers. *AIChE J.* **2013**, *59*, 3502−3513.
(40) Maheshwari, S.; Tsapatsis, M.; Bates, F. S. Synthesis and thermodynamic properties of poly(cyclohexylethylene-*b*-dimethylsiloxane-*b*-cyclohexylethylene). *Macromolecules* **2007**, *40*, 6638−6646.
(41) Dorgan, J. R.; Janzen, J.; Clayton, M. P.; Hait, S. B.; Knauss, D. M. Melt rheology of variable L-content poly(lactic acid). *J. Rheol.* **2005**, *49*, 607.
(42) Dorgan, J. R.; Williams, J. S.; Lewis, D. N. Melt rheology of poly(lactic acid): Entanglement and chain architecture effects. *J. Rheol.* **1999**, *43*, 1141−1155.
(43) Grijpma, D. W.; Penning, J. P.; Pennings, A. J. Chain Entanglement, Mechanical Properties and Drawability of Poly(lactide). *Colloid Polym. Sci.* **1994**, *272*, 1068−1081.
(44) We have determined the entanglement molar mass of PD to be 5.9 kg mol^{-1}. See Figure S12 of the Supporting Information for experimental details. Literature values for the entanglement molar mass for amorphous PLA in the literature are widely variable ($3.6 < M_e < 10.5$ kg mol^{-1}). This is further discussed in the Supporting Information.
(45) Drobny, J. G. *Handbook of Thermoplastic Elastomers*; Plastics Design Library; Elsevier Science: New York, 2007.
(46) Keller, A.; Pedemonte, E.; Willmouth, F. M. Macro-lattice from segregated amorphous phases of a three block copolymer. *Nature* **1970**, *225*, 538−539.
(47) Albalak, R. J.; Thomas, E. L. Microphase separation of block copolymer solutions in a flow field. *J. Polym. Sci., Part B: Polym. Phys.* **1993**, *31*, 37−46.
(48) Pakula, T.; Saijo, K.; Kawai, H.; Hashimoto, T. Deformation behavior of styrene-butadiene-styrene triblock copolymer with cylindrical morphology. *Macromolecules* **1985**, *18*, 1294−1302.